IOP Conference Series:
Materials Science and
Engineering

PAPER • **OPEN ACCESS**

The Mode Selector Mechanism (MSM): a bi-stable cryo-actuator operated at 4.2K

To cite this article: E. Lallemand *et al* 2025 *IOP Conf. Ser.: Mater. Sci. Eng.* **1327** 012163

The Mode Selector Mechanism (MSM): a bi-stable cryo-actuator operated at 4.2K

E. Lallemand[1*], T. Thibert[1], B. Marquet[1], J-Y. Plesseria[1], F. Henrotte[2], C. Geuzaine[2], L. Kiener[3], G. Lang[3], H. Saudan[3], N. Kalentics[3]

[1] CSL - Centre Spatial de Liège, Université de Liège, Liège, Belgium
[2] ACE - Applied and Computational Electromagnetics, Université de Liège, Liège, Belgium
[3] CSEM SA - Centre Suisse d'Electronique et de Microtechnique, Neuchâtel, Switzerland

[*]E-mail: etienne.lallemand@uliege.be

Abstract. A cryogenic environment implies a lot of constraints and uncertainties when it comes to the use of mechanical parts since the material properties are thermally dependent. This is even more true when the mechanical parts ensure the motion of a mechanism. In that context, the Centre Spatial de Liège (CSL) has developed a specific mechanism with 3D printed parts. The Mode Selector Mechanism (MSM) is a bi-stable cryo-actuator operated at 4.2 K developed by Centre Spatial de Liège. The MSM development started as part of the far-infrared spectrometer SAFARI on the ESA/JAXA SPICA space telescope. It is taking place now in the preparation and anticipation of next-generation cryogenic missions.

The MSM is characterized by its ability to switch between two stable positions an optical part, such as a mirror, at ambient as well as at cryogenic temperature (4.2 K). The particularity of this bi-stable actuator is a passive locking at both positions, to prevent electromagnetic interference sources. The actuator is also optimized regarding the energy dissipated during actuation. For that reason, specific elements such as magnets, copper coils, and flexible pivots, designed and 3D printed by CSEM, are included in the actuator.

In this talk, we present first the setup and results for the characterization of the main components at cryogenic temperature. We highlight the challenges and solutions implemented during the development of dedicated test benches for magnetic field, electrical resistance, and mechanical torque measurements adapted to cryogenic temperature. For instance, conduction was minimized between ambient and cold areas, and molecular conduction from Helium at low pressure was added during transients to improve test dynamics. We conclude with the characterization of the MSM mechanism at 4.2 K, including the time of commutation between both positions and the power consumption.

1. Introduction

The Mode Selector Mechanism (MSM) was part of the SPICA (SPace Infrared telescope for Cosmology and Astrophysics) mission before its cancellation in 2020. It was a proposed infrared space observatory with a large, actively cooled telescope. SPICA was the candidate for the next M5 mission. The MSM moves a flip mirror that will pick up either low or high-resolution beam and direct it into the instrument light path, i.e. towards the grating modules. This mechanism

must ensure an accurate and reliable positioning of the flip mirror in two fixed and stable positions (i.e. unpowered) (1).

As shown in Figure 1, the mirror is mounted on two flex pivots. For each position, a permanent magnet holds the rotor in contact with the metallic core of the mechanism to close the magnetic circuit. Two windings can be individually powered to generate a magnetic field to counteract the permanent magnet and bring the rotor toward the other position. As soon as the power is shut down the rotor stays in this other position thanks to the permanent magnet. The solid contact ensures a repeatable positioning of the mirror in its two operational positions. In operation, the MSM will be used in cryogenic conditions, down to 4.2 K.

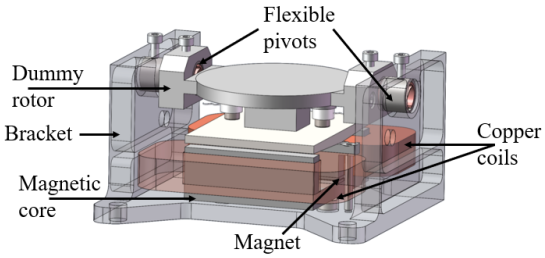

Figure 1. Prototype design of SPICA SAFARI Mode Selector Mechanism (MSM)

2. Characterization

2.1 Setup

Different elements of the MSM have been characterized individually inside the same cryostat refurbished for these specific needs. Here we will focus mainly on the measurement of the cryogenic stiffness.

The cryostat is presented in Figure 2. It is a double-wall cryostat, with a liquid helium tank protected by a liquid nitrogen thermal guard to limit thermal losses to the ambient area. The element to be characterized is instrumented inside a specific test cell under vacuum (Figure 2– 1). This cell is immersed in liquid helium (Figure 2– 2). The element under test is cooled mainly by the radiative exchange as it is under vacuum, but also by conduction when it is correctly thermalised to the cell walls. A low-pressure atmosphere of helium inside the test cell was used to boost thermal exchanges during transient phases at cryogenic temperature. For each subsystem, the test cell is modified for specific needs (2).

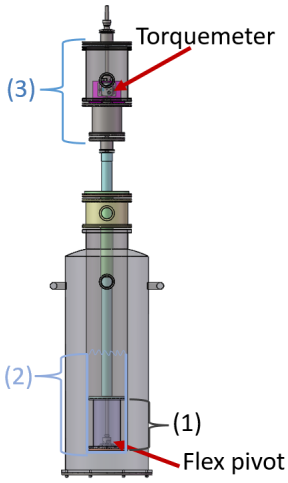

Figure 2. Cryostat used for subsystems characterization

2.2 Cryogenic stiffness

As the flexible pivots are key items since they ensure the rotation of the mirror, the characterization at cryogenic temperature was an important step of this study. The internal spring force of the pivots is used to reduce the needed energy during the commutation of the mechanism. CSL selected 316L stainless steel pivots printed with additive manufacturing by CSEM in Switzerland (Figure 3) (3).

Figure 3. Printed flexible pivot by CSEM

The pivot rotational stiffness was measured first at room temperature by CSEM. Then, CSL developed a specific test bench to measure the stiffness of these pivots at 4K. The mechanical

breadboard was developed to avoid all kinds of friction and to have high accuracy in the measurement of very low rotational stiffness (~0.01 N.mm/deg).

The pivot's stiffness is measured under vacuum and at cryogenic temperatures (Figure 2– 1, 2) while the torquemeter (Figure 4) is placed under vacuum at room temperature (Figure 2– 3) inside the cryostat. A rigid stainless steel transmission rod connects the pivot to the torquemeter. This rod is long enough to thermalize the cold extremity (4.2 K) while the other part remains at room temperature.

The view factor between cold and hot areas has been broken to radiatively isolate the torquemeter. Above the torquemeter, a command rod is used to control the flex pivot rotation from outside of the cryostat without vacuum leaks. Five-degree-of-freedom couplings are used on each side of the torquemeter to correct for slight misalignment and get rid of parasitic forces resulting from such misalignments. A system based on the principle of flexible double blades (Figure 5) has been developed to compensate for the differential contraction between the cryostat and transmission rod.

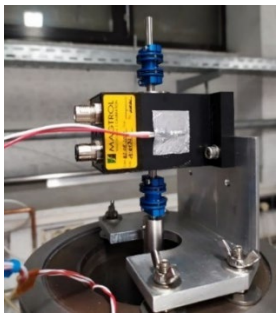

Figure 4. Torquemeter from Magtrol

Figure 5. Flexible pivot integrated with double spring blades

3. Mechanism characterization

3.1 Definition

After the characterization of the sub-elements, electromechanical analyses were performed with GetDP finite element solver (4) to predict the behavior of the MSM shown in Figure 1. During the conceptual design phase, the locking/unlocking torques required were calculated with margins of safety according to ECSS. The sizing locking torque has been used in the design phase as a target to optimize the magnet and magnetic core geometry. The sizing unlocking torque served to design the coils and associated actuation currents.

3.2 Experimental locking torque

The actual magnetic locking torque has been estimated with a direct measurement on the MSM prototype. This measurement was done at ambient conditions with an analogic torquemeter mounted in place of the flex pivots. As a result, the measured locking torque is estimated to 5.0e-2 ± 1.5e-2 N.m.

The result is in line with the design value of 3.7e-2 N.m. This validates the overall magnetic FEM modelling process. On the prototype, the flex pivots are implemented with a symmetrical deflection of +/-3°. We did observe that the prototype effectively locked on both positions, at ambient and cold conditions.

3.3 Unlocking torque and actuation current

In the laboratory, we observe the prototype actuation as soon as the magnetic locking force is nullified by the creation of an opposite magnetic field with the electro-magnet. The corresponding

current, which is the minimum current for actuation, is computed using experimental locking torque (Table 1). As the pivots are set in a neutral position in the prototype, the same current should be applied on both sides. This current serves as a reference in the commutation tests on the MSM prototype.

Table 1. Commutation current on MSM prototype (theorical)

Temperature	Commutation current (mA)
Ambient (293K)	4.4
Cryogenic (4.2K)	4.2

4. Results

4.1 Flex pivots

The stiffness of the printed pivot measured by CSEM is presented in Table 2. At 293K, a difference of 12% is observed between the CSEM measurements (3.88 N.mm/deg ±15%) and the CSL's one (4.38 N.mm/deg ±2%). This is acceptable as it is in the margin of error of CSEM measurements. At 77K and 4K, the stiffness is higher than at 293K, but it reduces between 77K and 4K. The stiffness of the pivots follows the Young modulus tendency as seen in Figure 6 where the blue dots represent the evolution of the measured pivot stiffness. Back at room temperature, the stiffness is recovered. The post-test visual inspection did not reveal any kind of premature aging. Furthermore, since the stiffness went back to its nominal value, we can conclude the absence of internal degradation.

Table 2. AM flex pivot stiffnesses measured at different temperatures

Stiffness condition	Manufacturer	CSL cryogenic BB					CSL simplified BB		
Temperature (K)	293	293	77	293	4.2	293	293		
Angular deformation (deg)	Theoretical	+/- 2°					+/- 2°	+/- 5°	+/- 2°
Stiffness (N.mm/deg)	3.88	4.36	4.66	4.45	4.65	4.38	4.30	4.27	4.31

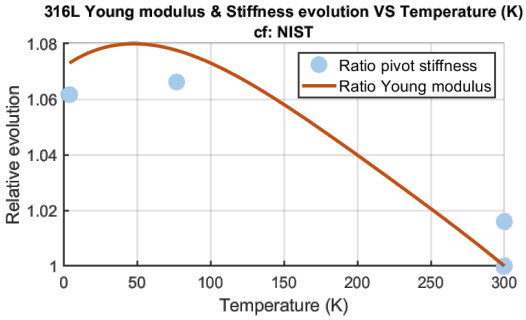

Figure 6. Young modulus evolution VS temperature (K) NIST data (orange curve) (5) and measured stiffness (blue spots)

4.2 MSM mechanism

4.2.1 Room temperature

Once integrated, the MSM's windings are supplied with current to switch the mechanism. At ambient conditions, the mechanism is connected to a power supply unit. The voltage is increased up to the commutation. The same is done in reverse. The model prediction (GetDP), the currents, and the voltages observed at the commutation are reported in Table 3. The resistances of the coils at ambient temperature are recalled in the table for completion.

Table 3. Electrical properties at ambient temperature to switch the MSM from one side to the other

Model prediction (GetDP)			Direction 1			Direction 2		
U (V)	I (mA)	R(Ohm)	U (V)	I (A)	R(Ohm)	U (V)	I (A)	R(Ohm)
17	0.0044	3870	14	0.004	3341	24	0.007	3271

We observe a good correlation between the measurements and the model predictions (4.4 mA), yet the power needed to switch the MSM prototype from one side to the other is not symmetrical. This is explained in one part by slight asymmetries in the mechanical assembly. The central magnetic leg with the magnets could be better positioned to have a perfectly symmetrical magnetic core. The alignment of the flex pivots with the rotation axis could be improved by tighter machining tolerances and the use of alignment pins in the rotating parts (mirror, anchor, pivots axes). On the other side, the difference in shape of the coils due to their prototype nature could impact the asymmetry. Indeed, due to this difference, the coils do not fit the same way on the magnetic core and so the magnetic field from the coils is not symmetrical.

4.2.2 Cryogenic temperature

For cryogenic needs, two switch contactors are added to the mechanism to follow the commutation of the MSM. Indeed, as it is in a closed environment, it is impossible to observe visually the commutation. An open circuit is measured when the switch is open, otherwise, a given resistance is measured. With this process we can identify the first time when the MSM starts to move (both contactors are open), and the final time when the commutation is finished (one contactor is closed). In addition, diodes DT-470 have been placed on each side of the mechanism to follow the temperature evolution. The coils were connected to the acquisition system to measure the resistance. They were also connected to the power supply (Figure 7).

The MSM is finally cooled down to 4.2 K. The resistance falls from ~3300 Ω to ~25 Ω, with the temperature. Therefore, the current limit was adjusted carefully. An oscilloscope is used to record the evolution of the current with time. Once the mechanism has commuted, the power supply is switched off manually. The measurements are repeated at different voltages for both directions.

Figure 8 shows the typical evolution of current and dissipated energy with time. At t0, the power supply is switched on. The current increases in the coil until the mirror takes off from its support. At this perfect moment, the magnetic loop generated by the magnets opens in the MSM magnetic core. It introduces an instantaneous reduction of the circuit inductance and so of the current during the transient phase until the mirror has completed its rotation. At this step, the power supply is switched off, with a slight delay as it is manually operated. When the power supply is switched off, the current starts to decrease quite slowly caused by the inductance discharge. The power and energy consumption are computed and integrated based on the current measurement during the actuation. The inductance is a key parameter in an RL circuit as its back-EMF limits the rate of change in the circuit current, in the form of a current in the circuit when the power supply is switched off. This discharge will so generate resistive power dissipation during the discharge phase. It is truer with this specific coil as it has a high number of windings, so a high inductance (6).

Table 4. Parameters for commutation at 4.2 K

	Voltage (V)	Current max (A)	Time to switch – ts (s)	Energy @ts (mJ)	Power @ts (mW)
Way in	12	0.005	0.26	0.15	0.69
Way back	12	0.005	0.28	0.17	0.62

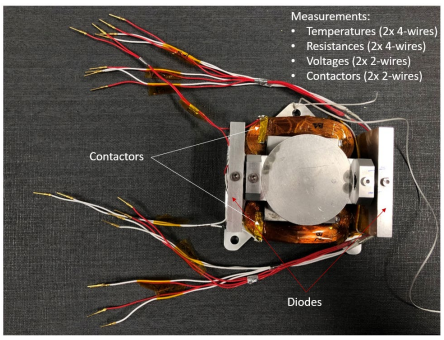

Figure 7. MSM with all the electrical connections for acquisition

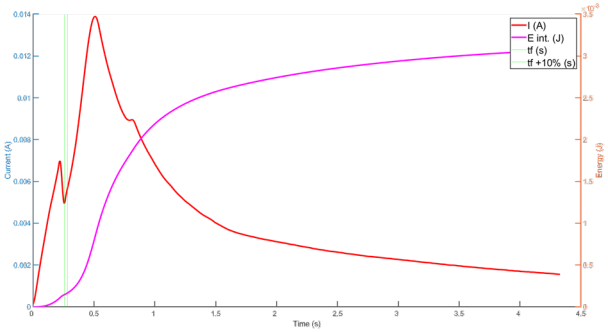

Figure 8. Trendline of energy dissipated @12 V, 4.2K

Table 4 shows parameters (current, time to switch, energy, and power dissipated) for 12 V. Results in both directions have the same order of magnitude and are aligned with the results of the magnetic finite element model. Therefore, the MSM seems symmetrical, as expected, and as observed at room temperature. The slight variation between both directions is explained due to the coils' properties which are not perfectly identic (28 Ω for one, 23 Ω for the other at 4.2K) as explained in the previous chapter. Finally, at ts (coil charging + time of commutation) the dissipated energy remains constant at 0.15 mJ. Considering the discharging phase of the coil right after ts (coil switch off), the total energy dissipated is equal to 0.3 mJ.

5 Conclusion

Under this project, CSL has developed a mechanism able to work in cryogenic conditions with low power consumption. The MSM has been experimentally characterized at prototype level and the results are aligned with the theoretical design. Finally, most of the specifications defined early in the project have been marked as compliant. Improvements are already foreseen, to ensure a fit alignment and to improve thermoelastic aspects.

References

1. Roelfsema PR, Shibai H, Armus L, Arrazola D, Audard M, Audley MD, et al. SPICA - A large cryogenic infrared space telescope: Unveiling the obscured universe. Publications of the Astronomical Society of Australia. 2018;35.
2. Randall F. Barron. Cryogenic Systems. 2e ed. Oxford University Press, editor. 1985.
3. Spanoudakis P, Kiener L, Cosandier F, Schwab P, Giriens L, Kruis J, et al. Large Angle Flexure Pivot Development for Future Science Payloads. 2019.
4. Geuzaine C. GetDP: a general finite-element solver for the de Rham complex. In: PAMM Volume 7 Issue 1 Special Issue: Sixth International Congress on Industrial Applied Mathematics (ICIAM07) and GAMM Annual Meeting, Zürich 2007. Wiley; 2008. p. 1010603–4.
5. NIST. Material Properties: 316 Stainless [Internet]. [cited 2024 Jul 24]. Available from: https://trc.nist.gov/cryogenics/materials/316Stainless/316Stainless_rev.htm
6. Théodore Wildi. Electrotechnique. 3e ed. Presses de l'université Laval, editor. 2000.

Acknowledgment

CSL would like to thank ESA and PRODEX office for the opportunity to work on this project with innovative solutions. It has been a rewarding experience in all areas of engineering.